Plant Physiol. (1973) 52, 531–538

S2B

A Mathematical Treatment of Munch's Pressure-Flow Hypothesis of Phloem Translocation[1,2]

Received for publication February 2, 1973

A. Lawrence Christy[3] and Jack M. Ferrier[4]
Department of Botany, Ohio State University, Columbus, Ohio 43210

ABSTRACT

The steady state solutions of two mathematical models are used to evaluate Münch's pressure-flow hypothesis of phloem translocation. The models assume a continuous active loading and unloading of translocate but differ in the site of loading and unloading and the route of water to the sieve tube. The dimensions of the translocation system taken are the average observed values for sugar beet and are intended to simulate translocation from a mature source leaf to an expanding sink leaf. The volume flow rate of solution along the sieve tube, water flow rate into the sieve tube, hydrostatic pressure, and concentration of sucrose in the sieve tube are obtained from a numerical computer solution of the models. The mass transfer rate, velocity of translocation, and osmotic and hydrostatic pressures are consistent with empirical findings. Owing to the resistance to water flow offered by the lateral membranes, the hydrostatic pressure generated by the osmotic pressure can be considerably less than would be predicted by the solute concentration. These models suggest that translocation at observed rates and velocities can be driven by a water potential difference between the sieve tube and surrounding tissue and are consistent with the pressure-flow hypothesis of translocation.

The generation of sufficient hydrostatic pressure to overcome the resistance to solution flow offered by the sieve tube and sieve plates remains a central problem in the consideration of Münch's pressure-flow hypothesis as the mechanism of translocation in the phloem. The hydrostatic pressure available to drive solution flow has been estimated from the concentration of solutes in sieve tube sap (22, 25). However, owing to resistance to water flow offered by the membranes between the sieve tube and surrounding tissue, the hydrostatic pressure in the sieve tube could be considerably less than the osmotic pressure predicted on the basis of sieve-tube-sap solute concentration.

A number of mathematical models have been formulated to describe translocation in the phloem (7, 9, 11, 17; see Reference 4 for review). However, most of these models have been concerned solely with the movement of radioactive tracers (2, 9, 11) and have not dealt with the osmotic and hydrostatic pressures in sieve tubes or the movement of water into and through sieve tubes. A recent attempt to quantify these aspects of the translocation process (8) failed to deal realistically with sieve tube anatomy, including the dimensions of the sieve tube, and ignored the presence of sieve plates. In addition, translocation is a continuous process, and a model attempting to simulate translocation should include continuous loading and unloading of translocate.

This paper describes two mathematical models based on irreversible thermodynamics that attempt to quantify the pressure-flow hypothesis of phloem translocation. These models can be used to predict the osmotic and hydrostatic pressure required to drive solution flow in sieve tubes and to evaluate the pressure-flow hypothesis as a plausible mechanism of translocation.

DESCRIPTION OF THE MODELS

Two models will be considered. In model I, sucrose is assumed to be actively loaded directly into the sieve tube and unloaded from the sieve tube (Fig. 1). In model II, accumulation and unloading are assumed to be accomplished by specialized phloem parenchyma cells adjoining the sieve tube, with free movement of solution between these cells and the sieve tube (Fig. 2). The translocation pathway is composed of three regions of equal length: a source region, a path region, and a sink region (Fig. 1). The basic model in both cases consists of a single sieve tube divided into sieve tube elements by sieve plates (Fig. 3) and surrounded by a reservoir the water potential of which (ψ_o) is −3 atm. The main difference between models I and II arises from the different membrane areas through which water can enter and leave the translocation pathway. The equations derived below apply to both models I and II.

The assumptions basic to the models are as follows: (*a*) Sucrose is actively loaded in the source region and actively unloaded in the sink region. In the path region loading and unloading of sucrose do not occur. (*b*) Flow both into and down the sieve tube can be described by linear equations involving hydrostatic and osmotic pressure gradients. The flow of water and solution in the models is passive, in that input of metabolic energy occurs only during active loading and unloading of sucrose. (*c*) The pores of the sieve plates are open (1, 5; Fisher, personal communication) and the conductance of each plate and the sieve-tube element can be calculated from Poiseuille's equation (18). (*d*) The reflection coefficient (σ) for sucrose was assumed to be unity for the lateral membrane and zero for the sieve plate.

The basic equation from irreversible thermodynamics for

[1] A portion of this work was conducted at the Department of Botany, University of Georgia, Athens, Ga.

[2] Paper 837 from the Department of Botany, Ohio State University, Columbus, O.

[3] Present address: Department of Botany, University of Georgia, Athens, Ga. 30601.

[4] Present address: Department of Physics, Ohio State University, Columbus, O. 43210.

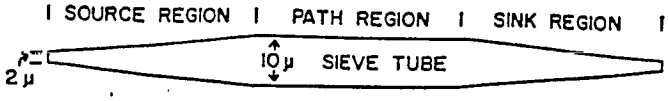

FIG. 1. Diagram depicting the sieve tube of Model I and the relationship of the source, path, and sink regions. Although it appears in this diagram that the sieve tube radius changes linearly in the source and sink region, in fact, it is the cross-sectional area which changes linearly with distance.

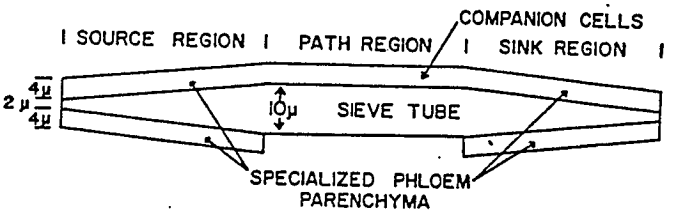

FIG. 2. Diagram depicting Model II and the relationship between the sieve tube, specialized parenchyma cells, and companion cells. Although it appears in this diagram that the sieve tube radius changes linearly in the source and sink region, in fact, it is the cross-sectional area which changes linearly with distance.

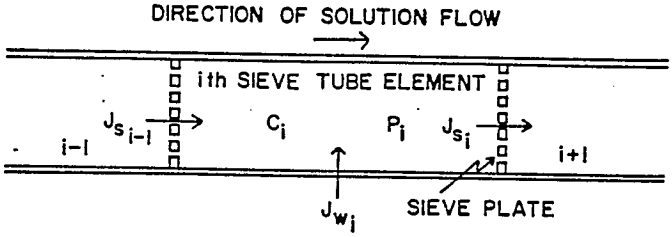

FIG. 3. Diagram of sieve tube element showing the computed variables and the relationship of the i^{th} element to the $i + 1$ and $i - 1$ elements.

volume flux, J ($cm^3 cm^{-2} sec^{-1}$), across a membrane is

$$J = L_p(\Delta P - \sigma\Delta\Pi) \quad (1)$$

where P is hydrostatic pressure in atm, π is osmotic pressure in atm, L_p is the membrane conductivity in $cm^3\ cm^{-2} sec^{-1} atm^{-1}$, and σ is the reflection coefficient for the solute (21). Since σ for sucrose is assumed to equal 1.0 for the lateral membranes, the flux of water from the reservoir into the ith sieve tube element (Fig. 3) is given by

$$J_{w_i} = L_p(\psi_0 - P_i + C_iRT) \quad (2)$$

where ψ_0 is the water potential in the reservoir; P_i and C_i are the hydrostatic pressure and sucrose concentration, respectively, in the ith sieve tube element; R is the gas constant; and T is the absolute temperature. The volume flux of the solution down the tube, from the ith element to the $i + 1$ element (Fig. 3), is given by

$$J_{s_i} = L_s(P_i - P_{i+1}) \quad (3)$$

assuming that $\sigma = 0$ and L_s is the conductivity of the sieve tube and plate.

Since water must be conserved, we have

$$J_{s_{i-1}}(1 - \alpha C_{i-1})A_{s_{i-1}} + J_{w_i}A_{p_i} = J_{s_i}(1 - \alpha C_i)A_{s_i} \quad (4)$$

where αC is the fraction of solution volume occupied by sugar, A_{s_i} is the sieve tube cross-sectional area in cm^2, and A_{p_i} is the lateral membrane surface area in cm^2 of the ith sieve tube element. By combining equations 2, 3, and 4, the hydrostatic pressure in the ith element can be calculated:

$$P_i = \frac{L_pA_{p_i}(\psi_0 + C_iRT) + L_sA_{s_{i-1}}(1 - \alpha C_{i-1})P_{i-1} + L_sA_{s_i}(1 - \alpha C_i)P_{i+1}}{L_pA_{p_i} + L_sA_{s_{i-1}}(1 - \alpha C_{i-1}) + L_sA_{s_i}(1 - \alpha C_i)} \quad (5)$$

the concentration in the ith element is given by

$$C_i(t + \Delta t) = C_i(t) + \frac{(r_i + J_{s_{i-1}}C_{i-1}A_{s_{i-1}} - J_{s_i}C_iA_{s_i})\Delta t}{V_i} \quad (6)$$

where r is the loading rate in $\mu g\ sec^{-1}$, t is time in sec, and V is volume in cm^3.

A steady state solution of equations 2, 3, 4, 5, and 6 was found by iterative numerical solution employing a Fortran program on an IBM 360 computer. Values for the constants L_p, L_s, and r were set as described below. Starting with zero or low values for the variables, $J_s = 0$, $J_w = 0$, $P = 0$ and $C = 5 \times 10^4$ μg of sucrose ml^{-1} (5%, w/v) in the source region, new values for C were calculated from equation 6. New values for the other variables were calculated using equation 5 for P, equation 3 for J_s, and equations 2 and 4 for J_w. This process was repeated many times, resulting in an asymptotic approach of the variables to their steady state values. When the translocation rate into the sink region is greater than 98% of the total loading rate (1.63×10^{-3} μg of sucrose sec^{-1}), additional computations result in insignificant changes in the variables, which are very close to their steady state values. No physiological significance can be attached to the variables during the approach to steady state because of the approximate nature of the calculations during that period. Therefore, although time is a variable in equation 6, only the time-independent steady state values can be considered as physiologically significant.

The dimensions of the translocation system taken are average observed values for sugar beet (12, 20) and are intended to simulate translocation from a mature source leaf to an expanding sink leaf. The length of the sieve tube elements are 200 μm; and the cross-sectional area increases in linear steps from 3.14 μm^2 to 78.5 μm^2 in the source, remains a constant 78.5 μm^2 in the path, and decreases from 78.5 μm^2 to 3.14 μm^2 in the sink (Figs. 1 and 2). The changes in cross-sectional area within the sink and source regions are based on Fisher's (11) observation of a linear relationship between leaf area and the cross-sectional area of the phloem servicing that leaf area. Geiger and Cataldo (12) found that 70 cm of minor vein serviced 1 cm^2 of sugar beet source leaf. Assuming that a petiole of sugar beet contains 350 sieve tubes (12), approximately 7 sieve tubes would service 1 cm^2 of a 50 cm^2 source leaf, or 10 cm of minor vein per sieve tube. In this model the source, path, and sink regions are each comprised of 480 sieve tube elements and are 9.6 cm long.

If the sieve tube elements are 200 μm long and 1 cm^2 of source leaf is serviced by 70 cm of minor vein (12), then there are 3500 sieve tube elements per cm^2 of source leaf. A translocation rate of 0.71 μg of sucrose $min^{-1}\ cm^{-2}$ of source leaf (3) yields a loading rate of 3.4×10^{-6} $\mu g\ sec^{-1}$ per sieve tube element. This value is used as the loading rate for each sieve tube element in the source region with a total loading rate of 1.63×10^{-3} $\mu g\ sec^{-1}$.

At the beginning of a computer solution the unloading rate was equal to 10% of the sugar in each sieve tube element per second. This was done only to minimize the time needed for reaching steady state and to prevent extreme fluctuations in the variables during computer computations; no physiological significance is implied by this condition. As the solution approached steady state, the unloading rate per sieve tube element in the sink was set equal to the loading rate per sieve tube element in the source, as is assumed to be the case at steady state.

In sugar beet, the average sieve plate pore diameter is 0.2 μm, with a plate thickness of 0.4 μm, and the total pore area is approximately 50% of the plate area (Geiger and Cataldo, unpublished data). Assuming a 15% sucrose solution (viscosity = 1.40×10^{-2} poise at 25 C), Poiseuille's equation (see Horwitz [18] for justification) yields a L_p for the sieve plate of 11.23 cm sec^{-1} atm^{-1}. In the path region, a sieve tube cross-sectional area of 78.5 μm^2 (diameter of 10 μm) and a sieve tube element length of 200 μm gives a L_p for the sieve tube element exclusive of sieve plates of 112.3 cm sec^{-1} atm^{-1}. Combining the L_p values for the sieve tube and plate results in a total L_p for the sieve tube element of 10.2 cm sec^{-1} atm^{-1} (see "Appendix"). As the cross-sectional area of the sieve tube (A_t) changes in the source and sink region, L_p of the sieve plate remains constant (assuming constant pore size and coverage), while L_p of the sieve tube changes with A_t. Since the sieve tube L_p is much greater than the sieve plate L_p, except at the extreme ends of the system, the total L_p for the sieve tube element is assumed to be constant. Thus, L_p remains constant for the entire translocation system and L_pA_t for each sieve tube element is directly proportional to A_t in the computer solution of the model. Modifying the model to include the effect of A_t on the sieve tube L_p results in insignificant changes in the calculated variables. However, this is true only because of the particular range of parameters used. With a larger range of A_t values or a smaller sieve tube L_p to sieve plate L_p ratio, total L_p could not be held constant in the source and sink regions.

Preliminary solutions with a small system indicated that the computer time required to obtain a steady state solution of this system increases with the square of the number of elements. To conserve computer time, the 1440 elements of the translocation system are divided into 120 sections with each section representing a series of 12 sieve tube elements. In effect, then, each section becomes a large sieve tube element with a L_p value and volume 12 times the L_p value and volume of the individual elements and L_s value 1/12 the average L_s value of the individual elements. Studies showed that the results of this system are in full agreement with a system of individual elements.

APPLICATION OF THE MODELS

Model I. Sucrose Loaded Directly into the Sieve Tube. Values for the volume flow rate of solution down the sieve tube ($J_{v,t}A_{s,t}$), of water flow rate into the sieve tube elements ($J_{w,t}A_{p,t}$), and of P and C obtained from a steady state solution of model I are plotted as a function of distance along the translocation system (Fig. 4). The value of L_p is assumed to be 5×10^{-7} cm sec^{-1} atm^{-1} and L_s is 10.2 cm sec^{-1} atm^{-1}. The osmotic and hydrostatic pressure gradients calculated for the path region are 12.0 and 7.1 atm m^{-1}, respectively, and the velocity (where velocity = volume flow rate/$A_{s,t}$) at the center of the path is 0.9 cm min^{-1}.

In the source region the volume flow rate along the sieve tube increases as more sugar and water enter the sieve tube (Fig. 4C). This increase would also occur in a plant, with the rate and amount of increase dependent on the branching of the minor vein in the source leaf. In the sink region the flow rate decreases as water and solute leave the sieve tube. Note that the velocity increases continually along the sieve tube (Fig. 4C). In the sink region, the cross-sectional area decreases faster than the volume flow rate, resulting in an increase in velocity.

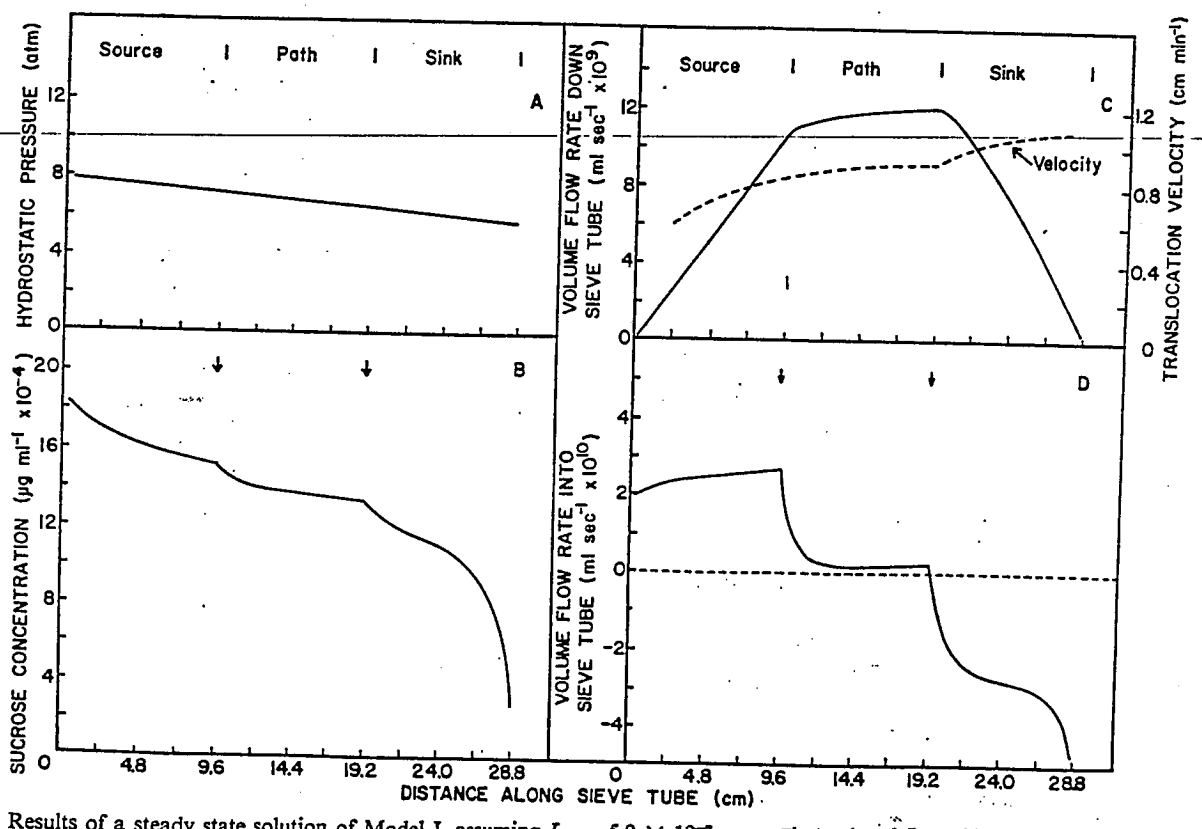

FIG. 4. Results of a steady state solution of Model I, assuming $L_p = 5.0 \times 10^{-7}$ cm sec^{-1} atm^{-1} and $L_s = 10.2$ cm sec^{-1} atm^{-1}. C: volume flow rate down the sieve tube (——) and velocity of the translocation stream (——); D: positive values indicate flow into the sieve tube and negative values indicate flow out of the sieve tube.

At the transition from loading in the source to no loading along the path, and then to unloading in the sink, marked changes occur in the concentration and volume flow rates into and along the sieve tube (Fig. 4, C and D). These changes would also be expected to occur in a plant depending on how sharp the transition is between the source, path, and sink and the unloading rate, if any, in the path.

Of the constants used to characterize the model, L_p is the most difficult to obtain satisfactory values for, but one of the most important in terms of its effects on the translocation system. For this reason, several solutions were obtained for model I with values of L_p ranging from 1×10^{-7} to 5×10^{-6} cm sec^{-1} atm^{-1} (Fig. 5). An increase in L_p facilitates the influx of water into the sieve tube, thus decreasing the sugar concentration. Since at steady state the translocation rate (*i.e.*, amount of sucrose translocated per unit time) is constant, compensatory changes must occur in the velocity and concentration (*i.e.*, velocity × area × concentration = constant). The increase in velocity at higher L_p values must be effected by an increase in the hydrostatic pressure gradient. As L_p increases, the difference between the osmotic pressure gradient and the hydrostatic pressure gradient decreases, because the required water potential difference across the lateral membrane is reduced.

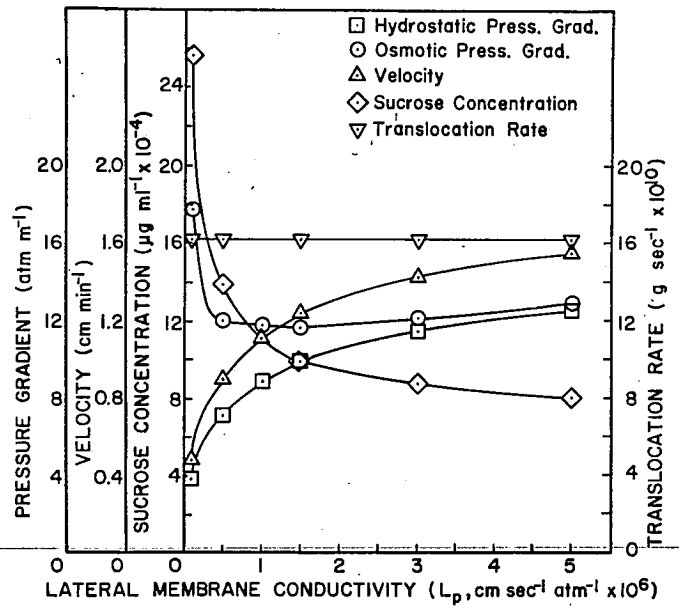

FIG. 5. Some important translocation parameters from steady state solutions of Model I as a function of lateral-membrane conductivity. The osmotic- (○) and hydrostatic-pressure gradients (□) in the path region, velocity (△), and concentration (◇) at the center of the path, and translocation rate (▽); L_s = 10.2 cm sec^{-1} atm^{-1}.

A number of variables may affect the value of L_s. For example, L_s will be affected by the sieve pore radius, the number of pores per sieve plate, and the number of sieve plates per unit length of sieve tube; and it might change sharply with callose deposition. To evaluate these effects on the behavior of the model, L_s was varied over a range of 5.1 to 20.4 cm sec^{-1} atm^{-1} (Fig. 6). An increase in L_s permits a higher flow rate down the sieve tube, resulting in compensatory changes in the velocity and concentration. Note that, although the velocity increases, there is still a decrease in the required pressure gradients (Fig. 6). As L_s increases, with L_p constant, the hydrostatic pressure gradient required to move the solution down the tube at a given velocity decreases, but the water potential difference across the lateral membrane required to move a given amount of water into the sieve tube remains constant. Thus, as L_s increases, both the hydrostatic and osmotic pressure gradients decrease, with the difference between the gradients approximately constant—but not quite, since there is an increase in the volume of solution moving down the sieve tube (Fig. 6). Except for the behavior of the pressure gradients, the model behaves in a qualitatively similar manner to an increase in either L_s or L_p.

Model II. Sucrose Loaded Initially into Parenchyma Cells. Using microautoradiography, several investigators (12, 23; Fisher, unpublished data) have demonstrated an accumulation of ^{14}C-photosynthate in pairs of specialized parenchyma cells immediately adjacent to the sieve tubes in minor veins. Geiger *et al.* (13) proposed that these specialized parenchyma cells could actively accumulate translocate followed by solution flow through the plasmodesmata from the specialized parenchyma cells to the sieve tube. To evaluate a loading mechanism of this type, model I was modified to include two companion cells in the source region and one companion cell in the path region (20) (Fig. 2). Because of a lack of data concerning the contact area and number and frequency of plasmodesmata between the specialized parenchyma cell and sieve tube element, the conductivity (L_p) between these two cells is set at infinity and the values of pressure and concentration are identical in both. This would not be an unreasonable assumption, since

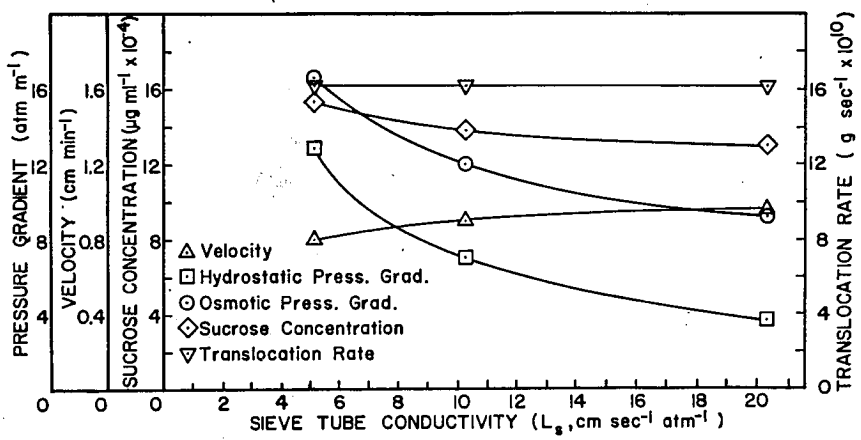

FIG. 6. Osmotic (○) and hydrostatic pressure gradients (□) in the path region, velocity (△) and concentration (◇) at the center of the path, and translocation rate (▽) as a function of sieve tube conductivity. Values are from steady state solutions of Model I, assuming L_p = 5.0×10^{-7} cm sec^{-1} atm^{-1}.

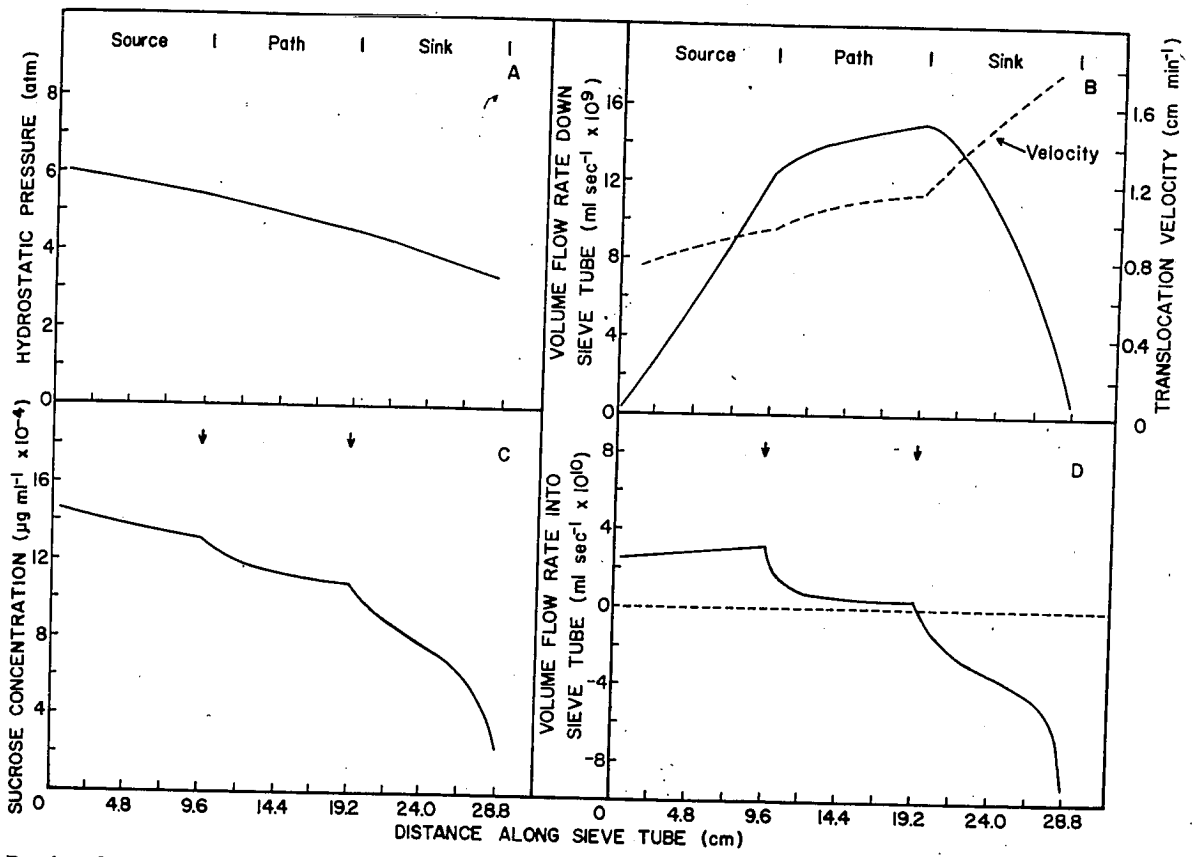

FIG. 7. Results of a steady state solution of Model II, assuming $L_p = 2.2 \times 10^{-7}$ cm sec^{-1} atm^{-1} and $L_s = 10.2$ cm sec^{-1} atm^{-1}. B: the volume flow rate down the sieve tube (——) and velocity of the translocation stream (----); D: positive values indicate flow into the sieve tube and negative values indicate flow out of the sieve tube.

L_s for the lateral membrane of the specialized parenchyma cells would presumably be less than L_p for the plasmodesmata (24).

Values for volume flow rate into and along the sieve tube and the pressure and concentration from the steady state solution of model II are not significantly different from the values obtained with model I (Figs. 4 and 7). However, the increase in lateral area presented to the bathing solution in model II required a L_p of 2.2×10^{-7} cm sec^{-1} atm^{-1} for the solution shown in Figure 7, which is somewhat lower than the L_p used for the solution of model I shown in Figure 4. The osmotic and hydrostatic pressure gradients calculated for the path region were 16.3 and 8.6 atm m^{-1}, respectively, assuming a L_s value of 10.2 cm sec^{-1} atm^{-1}. Note that in the solution of model II shown in Figure 7 more water is entering the sieve tube than in model I (Fig. 4), resulting in a higher velocity and a higher rate of increase in the velocity as compared to model I.

A further comparison of model I to II can be obtained by comparing the models at the same L_p value of 5.0×10^{-7} cm sec^{-1} atm^{-1} (Figs. 5 and 8). As a result of the higher A_p, the velocity and hydrostatic pressure gradient are higher and the concentration and osmotic pressure gradient are lower in model II than in model I. In addition, model II appears to be less sensitive to changes in L_p than model I (Figs. 5 and 8). When L_s is varied, similar results are obtained from both models (Figs. 6 and 9).

An analysis of the relationship between the osmotic and hydrostatic pressure gradients and L_p and L_s can be obtained from Figures 10 and 11. At a constant L_p, an increase in L_s has little effect on the difference between the hydrostatic and osmotic pressure gradients. However, with a constant L_s, an

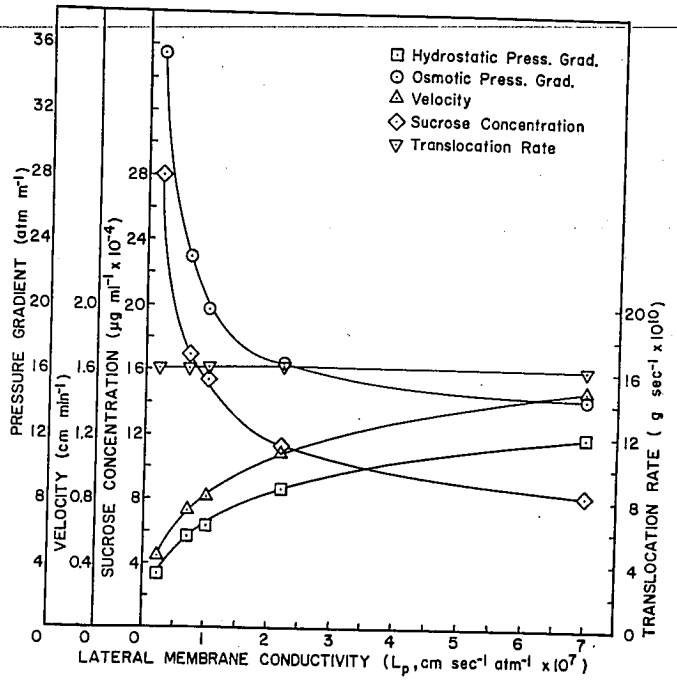

FIG. 8. Osmotic (○) and hydrostatic (□) pressure gradients in the path region, velocity (△) and concentration (◇) at the center of the path, and translocation rate (▽) as a function of lateral-membrane conductivity. Values are from steady state solutions of Model II, assuming $L_s = 10.2$ cm sec^{-1} atm^{-1}.

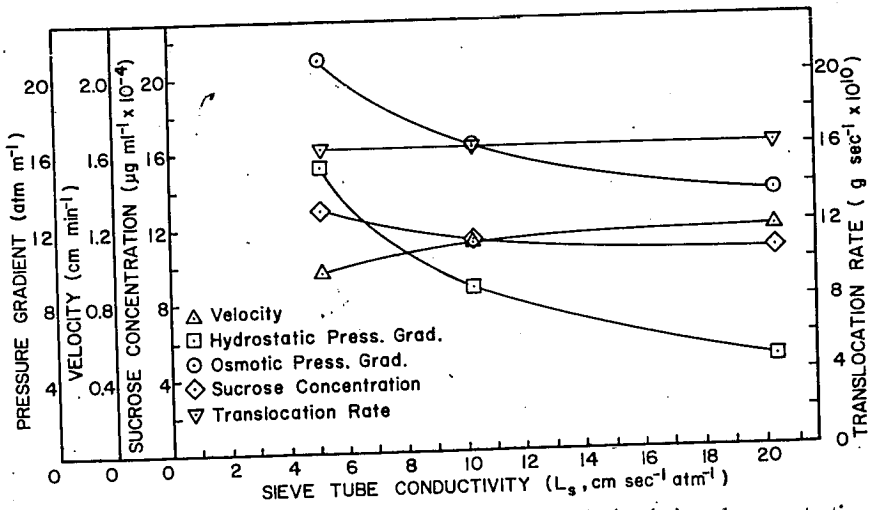

FIG. 9. Osmotic (○) and hydrostatic (□) pressure gradients in the path region, velocity (△) and concentration (◇) at the center of the path, and translocation rate (▽) as a function of sieve tube conductivity. Values are from steady state solutions of Model II, assuming $L_p = 1.0 \times 10^{-7}$ cm sec^{-1} atm^{-1}.

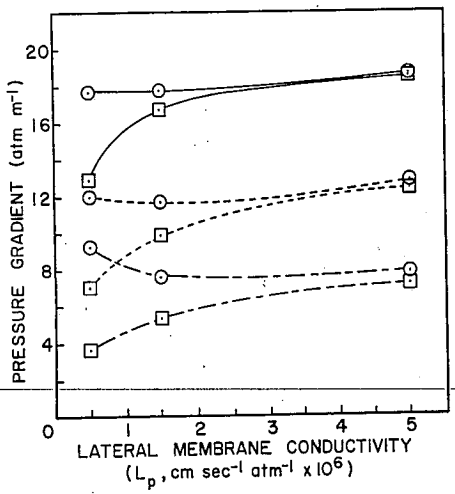

FIG. 10. Osmotic pressure gradient (○) and hydrostatic pressure gradient (□) in the path region as a function of lateral-membrane conductivity. Values are from steady state solutions of Model I, assuming $L_s = 5.1$ cm sec^{-1} atm^{-1} (——), $L_s = 10.2$ cm sec^{-1} atm^{-1} (-----), and $L_s = 20.4$ cm sec^{-1} atm^{-1} (— — —).

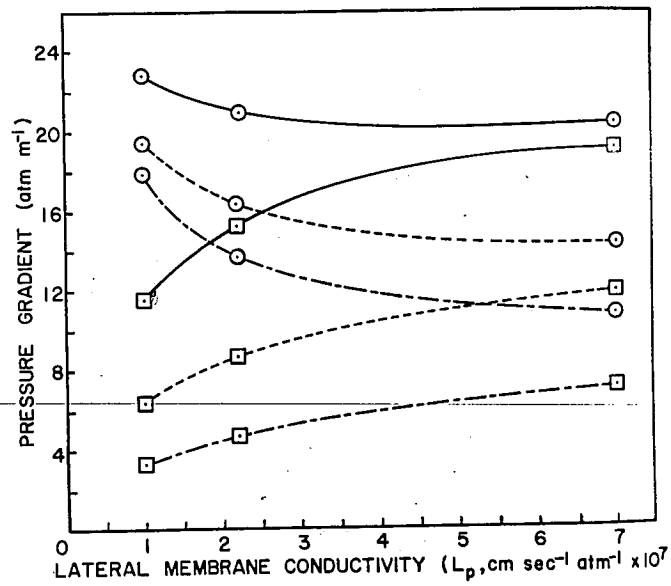

FIG. 11. Osmotic pressure gradient (○) and hydrostatic pressure gradient (□) in the path region as a function of lateral-membrane conductivity. Values are from steady state solutions of Model II, assuming $L_s = 5.1$ cm sec^{-1} atm^{-1} (——), $L_s = 10.2$ cm sec^{-1} atm^{-1} (-----), and $L_s = 20.4$ cm sec^{-1} atm^{-1} (— — —).

increase in L_p increases the hydrostatic pressure gradient (owing to the increase in velocity) while decreasing both the osmotic pressure gradient and the difference between the osmotic and hydrostatic pressure gradients (Figs. 10 and 11). Thus, the osmotic pressure gradient must be sufficient to overcome the resistance of the lateral membranes, sieve tube, and sieve plates, while the hydrostatic pressure gradient must be sufficient to overcome only the resistance of the sieve tube and sieve plates.

DISCUSSION

The results of the steady state solution of models I and II can be compared to empirical data to determine if the models adequately describe translocation in sieve tubes. It is evident from Table I that the translocation parameters predicted by the models are consistent with experimental findings. The hydrostatic pressure gradient in model I varied from 4 to 12 atm m^{-1} with a L_p of 1.0×10^{-7} to 5×10^{-6} cm sec^{-1} atm^{-1} and in model II varied from 3.5 to 12 atm m^{-1} with a L_p of 2.2×10^{-8} to 7.0×10^{-7} cm sec^{-1} atm^{-1} ($L_s = 10.2$ cm sec^{-1} atm^{-1}). Hammel (17) found a consistent but low hydrostatic pressure gradient in red oak. However, his measurements were made late in the growing season under questionable conditions for translocation and with senescence underway in the leaves. It is significant that the sieve tubes in both models have approximately the same dimensions as those found in sugar beet and function as a steady state translocation system with continual loading and unloading of sucrose.

The L_p values reported from plant cells vary depending on the methods used in their determination and the type of tissue studied. Dainty and Hope (6) reported a value of 9.3×10^{-9} cm sec^{-1} atm^{-1} for *Chara australis*. Tyree (24) calculated an L_p value from an earlier membrane study of 9.2×10^{-8} cm sec^{-1} atm^{-1} for *Salvinia aureculata*. Considering the experimental difficulties in determining L_p and the assumptions made in

the models, the range of L_p values used in models I and II appear reasonably consistent with empirically determined values. The additional resistance to water flow offered by the lateral membranes has not been considered in previous estimates of the resistance to water movement in the translocation system. The obvious importance of L_p in phloem translocation warrants further study of L_p values of sieve tubes and phloem parenchyma.

An important question concerning the pressure flow hypothesis has been the generation of sufficient hydrostatic pressure to overcome the resistance to solution flow. Eschrich *et al.* (8) reported that solution flow occurred in tubular semipermeable membranes in the absence of a hydrostatic pressure gradient and have proposed the term "volume flow" to describe the movement of solution in this system and in sieve tubes. Their intent in doing this was to focus attention on the site of energy input for driving solution flow. The emphasis on this point is perhaps justified, but their use of a new term to describe Münch's hypothesis (as subsequentlly modified by the discovery of active loading of sugars into the sieve tube [19]) seems unnecessary and somewhat confusing. One must assume that the sieve tube and sieve plates will offer a significant resistance to solution flow and, therefore, that a pressure gradient would exist in the presence of mass flow. As shown in equation 3, the volume flux of solution (J_s) across a sieve plate should be directly proportional to L_p and the hydrostatic pressure difference across the sieve plate (ΔP). The arrangement of sieve plates in a series as in a sieve tube would then result in a hydrostatic pressure gradient along the sieve tube. If the assumption were made that solution flow could occur in the absence of a hydrostatic pressure gradient, this would be tantamount to assuming zero viscosity. In addition, that movement of water into the sieve tube occurs as a consequence of solute loading has been an accepted aspect of Münch's pressure-flow hypothesis for many years. Thus there is little to be gained by referring to the same mechanism of translocation by another name.

Water movement in the translocation system is controlled by the water potential difference between the sieve tube and surrounding tissue. The water potential in the sieve tube in the source region must be low enough relative to the water potential in the surrounding tissue to move water across the lateral membranes into the sieve tube. In the sink region, the water potential in the sieve tube must be greater than in the surrounding tissue to move water out of the sieve tube across the lateral membrane. In addition, the water potenial in the sieve tube along the path will not be in thermodynamic equilibrium with the water potential in the surrounding tissue. Thus, if the water potential in the surrounding tissue is the same along the entire sieve tube, the osmotic pressure gradient in the sieve tube will be greater than the corresponding hydrostatic pressure gradient (Figs. 10 and 11). This difference between the osmotic and hydrostatic pressure gradients would be even greater when the water potential in the surrounding tissue in the sink region is greater than in the source region. This would be normal in a plant with mature leaves serving as the source region and the roots serving as the sink region. In both of the above situations, the lower the lateral membrane conductance, the larger the difference will be between the osmotic and hydrostatic pressure gradients (Figs. 10 and 11). The osmostic pressure gradient in the sieve tube could be less than the hydrostatic pressure gradient when the water potential in the surrounding tissue in the source region is greater than in the sink region. This could occur when mature source leaves are supplying translocate to immature sink leaves higher on the plant. In the latter case the water potential gradient in the surrounding tissue would be assisting in driving translocation, and the osmotic pressure gradient would provide only a portion of the motive force for solution flow, while in the two previous cases the osmotic pressure gradient provides all the motive force for solution flow[5].

Table I. *Comparison of Data from Models I and II with Empirical Data over a Range of L_p Values and a Constant L_s of 10.2 cm sec^{-1} atm^{-1}*

All values from the models were taken at the center of the path.

	Model I[1]	Model II[2]	Empirical Data	Reference
Velocity (cm min^{-1})	0.48–1.55	0.45–1.48	0.9	(14)
			0.4–1.9	(3, 15)
Concentration (%)	8.0–25.6	8.3–28.0	8.8	(10)
			10–25	(4)
Osmotic pressure (atm)	5.7–18.0	6.0–20.1	18.04	(10)
			20–24	(17)
Hydrostatic pressure (atm)	2.7–15.3	2.9–16.5	15–20	(17)
Specific mass transfer rate (g hr^{-1} cm^{-2} sieve tube)	7.3	7.3	4.8	(14)
			6–18[3]	(26)

[1] L_p from 1.0×10^{-7} to 5.0×10^{-6} cm sec^{-1}.
[2] L_p from 2.2×10^{-8} to 7.0×10^{-7} cm sec^{-1} atm^{-1}.
[3] Assuming that 20% of the phloem is sieve tubes.

Models I and II differ only in the site of loading and in the path of water from the xylem to the sieve tube. The accumulation of label in the specialized parenchyma cells of minor veins (12, 23; Fisher, unpublished data), and the presence of large-branched plasmodesmata between these cells and the sieve tube elements (7, 13) would tend to support model II. However, additional information is needed concerning vein loading and intercellular translocation of photosynthate in leaves, and the size and frequency of plasmodesmata between the sieve tube and the specialized phloem parenchyma cells.

Models I and II demonstrate that the hydrostatic pressure required to drive solution flow in sieve tubes at observed velocities and mass transfer rates can be produced by the water potential difference between the sieve tube and surrounding tissue. It appears that these mathematical models may adequately describe translocation in sieve tubes and support Münch's pressure-flow hypothesis as a plausible mechanism of translocation, at least over shorter distances. However, this support must be qualified in several respects. The models establish the potential importance of membrane conductivity to a pressure-flow mechanism and demonstrate that the hydrostatic pressure which can be generated by a given osmotic pressure may be much less than the osmotic pressure, rather than equal to it, as is conventionally assumed. Both of these factors further complicate the recognized difficulty of explaining translocation over long distances, such as occurs in trees.

Acknowledgments—The authors wish to thank D. B. Fisher for his helpful discussions, suggestions, and critical review of the manuscript. We are indebted to the Computer Center of the Ohio State University for the generous use of their facilities.

[5] One can speculate that an active transport of sugar from the sieve tube to the specialized parenchyma cells could produce a considerably higher osmotic pressure in these parenchyma cells than in the sieve tube. Thus, the flow of water through the plasmodesmata into the sieve tube in the source region would be independent of the osmotic pressure in the sieve tube, resulting in a pseudo-active loading of water and the generation of large hydrostatic pressures.

LITERATURE CITED

1. Anderson, R. and J. Cronshaw. 1970. Sieve-plate pores in tobacco and bean. Planta 91: 173–180.
2. Canny, M. J. and O. M. Phillips. 1963. Quantitative aspects of a theory of translocation. Ann. Bot. (N.S.) 27: 379–402.
3. Christy, A. L. 1972. Translocation kinetics in relation to source-leaf photosynthesis and carbohydrate concentration in sugar beet. Dissertation. Ohio State University, Columbus.
4. Crafts, A. S. and C. E. Crisp. 1971. Phloem Transport in Plants. W. H. Freeman Co., San Francisco.
5. Cronshaw, J. and R. Anderson. 1969. Sieve plate pores of *Nicotiana*. J. Ultrastruct. Res. 27: 134–148.
6. Dainty, J. and A. B. Hope. 1959. The water permeability of cells of *Chara australis* R. BR. Aust. J. Biol. Sci. 12: 136–145.
7. Esau, K. 1969. The Phloem. Gerbrüden Borntraegen, Berlin.
8. Eschrich, W., R. F. Evert, and J. H. Young. 1972. Solution flow in tubular semipermeable membranes. Planta 107: 279–300.
9. Evans, N. T. S., M. Ebert, and J. Moorby. 1963. A model for the translocation of photosynthate in the soybeans. J. Exp. Bot. 14: 221–231.
10. Fife, J. M., C. Price, and D. C. Fife. 1962. Some properties of phloem exudate collected from root of sugar beet. Plant Physiol. 37: 791–792.
11. Fisher, D. B. 1970. Kinetics of C-14 translocation in soybean. III. Theoretical considerations. Plant Physiol. 45: 119–125.
12. Geiger, D. R. and D. A. Cataldo. 1969. Leaf structure and translocation in sugar beet. Plant Physiol. 44: 45–54.
13. Geiger, D. R., J. Malone, and D. A. Cataldo. 1971. Structural evidence for a theory of vein loading of translocate. Amer. J. Bot. 58: 672–675.
14. Geiger, D. R., M. A. Saunders, and D. A. Cataldo. 1969. Translocation and accumulation of translocate in the sugar beet petiole. Plant Physiol. 44: 1657–1665.
15. Geiger, D. R. and S. A. Sovonick. 1970. Temporary inhibition of translocation velocity and mass transfer rate by petiole cooling. Plant Physiol. 46: 847–849.
16. Ginsburg, H. and B. Z. Ginzburg. 1970. Radial water and solute flows in roots of *Zea mays* I. Water flow. J. Exp. Bot. 21: 580–592.
17. Hammel, H. T. 1968. Measurement of turgor pressure and its gradient in the phloem of oak. Plant Physiol. 43: 1042–1048.
18. Horwitz, L. 1958. Some simplified mathematical treatments of translocation in plants. Plant Physiol. 33: 81–93.
19. Kursanov, A. L. 1963. Metabolism and transport of organic substances in the phloem. Advan. Bot. Res. 1: 209–278.
20. Sokolova, S. V. 1968. Fine structure of petiole phloem cells of *Beta vulgaris* L. Fiziol. Rast. 15: 757–763.
21. Stein, W. D. 1967. The Movement of Molecules across Cell Membranes. Academic Press, New York.
22. Tammes, P. M. L., J. Van Die, and T. S. Ie. 1971. Studies on phloem exudation from *Yucca flaccida* Haw. VII. Fluid mechanics and exudation. Acta Bot. Néer. 20: 245–252.
23. Trip, P. 1969. Sugar transport in conducting elements of sugar beet leaves. Plant Physiol. 44: 717–725.
24. Tyree, M. T. 1970. The symplast concept: a general theory of symplastic transport according to the thermodynamics of irreversible processes. J. Theor. Biol. 26: 181–214.
25. Weatherley, P. E. and R. P. C. Johnson. 1968. The form and function of the sieve tube. Int. Rev. Cytol. 24: 149–192.
26. Zimmermann, M. H. 1968. Translocation velocity and specific mass transfer in sieve tubes of *Fraxinus americana* L. Planta 84: 272–278.

APPENDIX

SYMBOLS

J_w = volume flux of water into the sieve tube ($cm^3\ cm^{-2}\ sec^{-1}$)
J_s = volume flux of solution down the sieve tube ($cm^3\ cm^{-2}\ sec^{-1}$)
L_p = lateral membrane conductivity ($cm\ sec^{-1}\ atm^{-1}$)
L_s = sieve tube conductivity ($cm\ sec^{-1}\ atm^{-1}$)
A_p = lateral membrane surface area (cm^2)
A_s = sieve tube cross-sectional area (cm^2)
σ = reflection coefficient
C = concentration ($\mu g\ cm^{-3}$)
P = hydrostatic pressure (atm)
π = osmotic pressure (atm)
R = gas content ($atm\ \mu g^{-1}\ cm^3\ °K^{-1}$)
T = absolute temperature (°K)
α = sucrose solution volume ($cm^3\ \mu g^{-1}$)
ψ_0 = water potential in surrounding reservoir (atm)
r = loading rate per sieve tube element ($\mu g\ sec^{-1}$)
V = volume (cm^3)

CALCULATION OF SIEVE TUBE CONDUCTIVITY

From Poiseuille's equation the sieve plate conductivity in $cm^3\ dyne^{-1}\ sec^{-1}$ is given by:

$$L_s(\text{plate}) = F\frac{r^2}{8\eta l}$$

where F is the fraction of the plate area covered by pores, r is the pore radius in cm, l is the sieve plate thickness in cm, and η is viscosity in poise. The sieve tube conductivity is given by:

$$L_s(\text{tube}) = \frac{R^2}{8\eta L}$$

where R is the radius of the tube and L is the length of the sieve tube element in cm. The total conductivity of one sieve tube element is given by:

$$L_s(\text{total}) = (L_s^{-1}(\text{tube}) + L_s^{-1}(\text{plate}))^{-1}$$

To convert L_s to units of $cm\ atm^{-1}\ sec^{-1}$, multiply by 0.987×10^{-6} $dyne\ atm^{-1}\ cm^{-2}$.